Azido-Coated Nanoparticles: A Versatile Clickable Platform for the Preparation of Fluorescent Polystyrene Core–PAMAM Shell Nanoparticles

ARTICLE · JANUARY 2012

READS
52

6 AUTHORS, INCLUDING:

Guillaume Rousseau
Claude Bernard University Lyon 1
14 PUBLICATIONS **102** CITATIONS
SEE PROFILE

Krystyna Baczko
Université de Versailles Saint-Quentin
21 PUBLICATIONS **247** CITATIONS
SEE PROFILE

Emmanuel Allard
Université de Versailles Saint-Quentin
27 PUBLICATIONS **441** CITATIONS
SEE PROFILE

Chantal Larpent
Université de Versailles Saint-Quentin
78 PUBLICATIONS **1,458** CITATIONS
SEE PROFILE

Macromolecules

Article

pubs.acs.org/Macromolecules

Azido-Coated Nanoparticles: A Versatile Clickable Platform for the Preparation of Fluorescent Polystyrene Core–PAMAM Shell Nanoparticles

Guillaume Rousseau, Hélène Fensterbank, Krystyna Baczko, Manuel Cano, Emmanuel Allard,* and Chantal Larpent

Institut Lavoisier de Versailles UMR-CNRS 8180, Université de Versailles-Saint-Quentin-en-Yvelines, 45 avenue des Etats-Unis, 78035 Versailles cedex, France

Supporting Information

ABSTRACT: The convergent synthesis of fluorescent polystyrene core–PAMAM shell nanoparticles in the 15–20 nm diameter range is presented using azido-coated nanoparticles (NP_{N3}) as a clickable platform. The coupling of the different partners occurs exclusively on the surface of the cross-linked polystyrene matrix owing to its nonswelling properties in water. PAMAM dendrons having an alkyne moiety at their focal point and peripheral carboxylic acid groups were covalently attached to the surface of azido-coated nanoparticles via a CuAAC reaction. Given the high density of azide anchoring groups on the NP surface (about 560 N_3 per NP) and the size of the PAMAM derivative, the grafting of dendrons was not complete, leaving azide units available for further functionalization with an alkyne dansyl derivative. These new dendron-coated nanoparticles, which possess a number of terminal functional groups comparable to the high eighth generation of PAMAM dendrimers, are obtained in a few steps without tedious chromatographic purification. Dendritic shell saturation levels of 70–85% were reached for these dendron-coated nanoparticles. The colloidal stability of the resulting scaffold was governed by the dendritic shell. Particularly, a pH-dependent electrostatic self-assembly process between the ammonium moieties of the cationic surfactant and carboxylate groups of PAMAM can be switched. This straightforward strategy gives access to dendron-coated nanoparticles as valuable building blocks for the construction of functional nanomaterials.

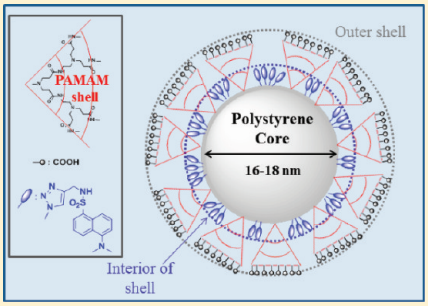

INTRODUCTION

Nanoparticles have attracted considerable interest over the past decade due to their unique physical and chemical properties that can be exploited in a wide range of applications such as in materials science[1] and biology.[2] Most of these applications require careful design of the nanoparticles and reliable strategies for constructing functional nanomaterials. Indeed, the properties of NPs are not only governed by their composition but are also influenced by their surface constitution. For example, many practical applications of inorganic nanoparticles require covering their surface with ligands to prevent NP aggregation, ensuring that their properties do not change, as well as to provide handles for convenient peripheral functionalization. The surface functionalization can be achieved through the use of polymers,[3] surfactants,[3,4] dendrimers, and other dendritic structures.[5]

Dendrimers and dendrons are the most intensely investigated subset of dendritic polymers.[6,7] Dendrimers are well-defined, monodispersed, three-dimensional macromolecules with a definite molecular weight. They contain three basic architectural components: a core, an interior of shells (generations) consisting of repeating branch-cell units, and terminal functional groups (the outer shell or periphery). The properties of dendrimers are dominated by the very high density of peripheral functional groups, although the internal cavities are also of a great significance due to their ability to encapsulate molecules or ions. Dendrons are associated with dendrimers since they represent a structural component of the parent dendrimer. Dendrons differ from dendrimers in their structure by their bifunctional nature. They possess a focal point that is functionalized differently than the periphery. This focal point allows dendrons to be grafted onto other molecules or solid supports.

Dendrimers are used as nanoreactors for templating metal nanoparticles leading to so-called dendrimer-encapsulated nanoparticles[8] (DENs) as well as surfactants adsorbing on the growing inorganic NPs affording dendrimer-stabilized nanoparticles (DSNs).[5] As far as dendrons are concerned, they can be associated with NPs through (i) direct ligand exchange processes,[9] (ii) direct-capping syntheses,[10] or (iii) covalent linkage.[11]

In parallel to the development of inorganic NPs, polymer nanoparticles have received considerable interest because well-documented polymerization techniques in microheterogeneous

Received: January 17, 2012
Revised: March 9, 2012
Published: April 6, 2012

media can provide control over the size, charge, functionality, and colloidal stability.[12] Numerous particles incorporating functionalities on the surface and/or within the polymer core have been produced for a variety of applications.[13,14] In particular, the polymerization of hydrophobic monomers in an oil-in-water microemulsion was found to give access to stable aqueous suspension of well-defined ultrafine particles, so-called nanolatexes, in the nanosized diameter range (15−30 nm).[15] We have recently reported two strategies to prepare aqueous suspension of azido-functionalized polystyrene nanoparticles using this technique.[16] The two synthetic routes developed in this work led to structurally different nanoparticles in the 15−20 nm diameter range with azide groups located only on the surface (postfunctionalization route) or distributed in the core and on the surface (copolymerization route). The high surface-to-volume ratio of these nanometer-sized particles provides remarkable accessibility of the functional groups, ensuring multiple anchoring sites on the NPs surface. The grafting of hydrophobic and hydrophilic alkynes derivatives was particularly efficient using CuAAC reaction. Moreover, compared to previously clickable polymeric nanomaterials reported in the literature,[17] cross-linked polystyrene-based NPs are not swollen in water. Thus, the coupling of alkynes through CuAAC reaction can be performed only on the NPs surface, leaving the particle core available for further functional arrangements. We believe that these structurally programmed azide-functionalized NPs are promising clickable platforms for the synthesis of functional nano-objects, especially for the design of new dendronized polystyrene nanoparticles.

Chemical modification of polymer nanoparticles with dendrimers or dendrons has been scarcely studied. Hawker and Wooley reported a series of researches on the preparations of shell or core cross-linked nanoparticles from amphiphilic polymers assembled into micelles.[18] They used multifunctional dendritic cross-linkers that give rise to the simultaneous stabilization of supramolecular assemblies and the introduction of reactive groups within the shell or core domain. Gillies and co-workers have recently described a new approach for the surface functionalization of vesicles assembled from polymers with dendrons having alkyne moieties at their focal point via a Cu(I)-catalyzed azide and alkyne cycloaddition reaction.[19] This study reveals that the use of dendritic scaffolds to display peripheral biological ligands on the polymer surfaces leads to an enhanced binding affinity of these ligands. As the micrometer-scale sizes of these vesicles were unsuitable for in-vivo circulation, Gillies et al. further explored the development of micelles and vesicles conjugated to dendrons functionalized with peripheral amines, guanidines, or hydroxyl groups in the nanoscale range.[20] Larpent and co-workers have previously reported the postfunctionalization of already formed NPs with a phosphorus containing dendron to give dendronized NPs[21] as well as with polypropylenimine (PPI) dendrimer to afford polyaminodendrimer-coated NPs.[22] These studies have shown that the properties and reactivity in solution of the resulting NPs were governed by the dendritic shell. The polyaminodendrimer-coated NPs were also functionalized with various dyes and led to colored nanolatexes.[22]

Owing to the efficiency of the click CuAAC reaction on the azide NPs,[16] we decided to assess the grafting of dendrons onto the surface of azide-functionalized nanoparticles obtained from the postfunctionalization route. We can expect that given the high density of azide units on the surface of NP and the large size of dendrons, the grafting should not be complete. This should afford giant dendrimer-like particles[21] in which surface modification through peripheral moieties of the dendrons could be envisioned via self-assembling processes or covalent linkages. Unlike the polyaminodendrimer-coated NPs in which the surface functionalization is limited at this point to the PPI surface dendrimer,[22] modification of our nano-objects should not be limited to the dendron surfaces but could be extended at will to the surface of the polystyrene core via the residuals azide units.

Herein, we describe the preparation of core−shell functional nanostructures in the 15−20 nm diameter range by covalent attachment of a PAMAM dendron having an alkyne moiety at its focal point and peripheral carboxylic acids to azide coated polystyrene-based NP surfaces using CuAAC reaction.[23,24] The azido-coated nanoparticles were prepared using the post-functionalization route. Cross-linked polystyrene nanoparticles are not swollen in water. Therefore, the functionalization within the nanoparticles cannot occur. Dendrons have been preferred to dendrimers because their structure possesses a focal point that is functionalized differently than the peripheral moieties. Their focal point allows dendrons to be grafted onto the nanoparticles surface and stand the carboxylic acid units free for further surface functionalization. The use of dendrons also prevents the interparticle linkages which can be observed with dendrimers coated nanoparticles. Given the high density of azide anchoring groups on the NP surface as well as the size of PAMAM dendrons, the grafting of the dendron is not complete, leaving azide units located around the core. The nano-objects thereby obtained possess three basic architectural components: a polystyrene core bearing azide units on its surface, a PAMAM shell, and peripheral functional groups (the outer shell). This efficient strategy allows the synthesis of giant dendrimer-like particles from nanolatexes using earlier generations of PAMAM dendrons. Dendron-coated nanoparticles are obtained in a few steps without tedious chromatographic purification. Dendritic shell saturation levels of 70−85% were reached in these nano-objects in which the availability and reactivity of the remaining azides has been demonstrated by grafting a dansyl derivative.

EXPERIMENTAL SECTION

Materials. Dodecyltrimethylammonium bromide (DTAB, Fluka, 98%), sodium azide (Acros, 99%), copper(II) sulfate anhydrous (Fischer, 98%), sodium ascorbate (Acros, 99%), propargylamine hydrochloride (Sigma-Aldrich, 95%), dansyl chloride (Alfa-Aesar, 99%), methyl acrylate (Acros, 99%), and ethylenediamine (Fluka, 100%) were used as received. Triethylamine (Acros, 99%) was distilled under nitrogen before use. Dichloromethane was dried and distilled under CaH_2 prior to use. All other solvents were used as received. MilliRo Water and Milli-Q water were used for microemulsion polymerization and sample dilution, respectively.

PAMAM derivatives **1**-($G_{0.5}$) and **3**-($G_{1.5}$)[25] and dansyl derivative **5**[16] were prepared according to the previously published procedures.

Measurements. ^{1}H NMR and ^{13}C NMR spectra were recorded using a Bruker AM300 spectrometer at 300 MHz (^{1}H) and at 75 MHz (^{13}C) in DMSO-d_6 or $CDCl_3$. Chemical shifts δ were referenced to internal solvent $CDCl_3$ (7.27 and 77.00 ppm) or DMSO-d_6 (2.50 and 39.50 ppm).[26]

ESI-MS mass spectra were obtained with a Waters Xevo Qtof. The infrared spectra were recorded using a FTIR apparatus (Nicolet 550). Elemental analyses have been obtained from the Service Central d'Analyze (CNRS, Vernaison, France) and the Service de Microanalyse (ICSN, Gif-sur-Yvette, France). UV/vis analyses were performed on a Perkin-Elmer spectrophotometer UV/vis/NIR Lambda 19. Steady-state fluorescence measurements were recorded

on a spectrofluorimeter FluoroMax-3 equipped with a 150 W xenon lamp and a slit width of 5 nm. For all measurements the samples were diluted so that the maximum of absorbance is less than 0.1 to avoid reabsorption artifact. The mean hydrodynamic diameter and the polydispersity index (PDI) of the nanoparticles were measured by quasi-elastic light scattering (QELS) with a Brookhaven 90Plus. PDI ≤ 0.100 corresponds to reasonably narrow monomodal distribution latexes. The samples were diluted 100 times in MilliRo water and then filtered through a 0.22 μm membrane to remove dust. For each sample, the measurement was performed three times at a temperature of 25 °C with a detection angle of 90°. AFM measurements were made using tapping mode operation with a Digital Instrument 3100 and a Nanoscope IIIa controller. Tapping mode etched silicon probes from Veeco (TESP-SS, spring constant k_0: 20−80 N m^{-1} and constant force f_0: 300−371 kHz) with a 3.5−4.5 nm radius of curvature were used. Mica substrates were prepared by cleaving to produce a smooth surface prior to sample deposition. The nanolatexes were diluted 4 × 10^4 times in water (so that the final concentrations of nanoparticles and surfactant were respectively 2.25 × 10^{-4} and 2.5 × 10^{-4} g L^{-1}). 10 μL of the dilute solutions was deposited on 9 mm mica disks and allowed to dry at room temperature for 12 h. AFM images were analyzed using WSxM software 5.0 Develop 4.2.[27]

Dialyses were performed using either Spectra/Por regenerated cellulose membranes with 12 000−14 000 g mol^{-1} molecular weight cutoff (MWCO) or an ultrafiltration device (Vivascience, Vivaspin concentrator 20, PES) with a 50 000 g mol^{-1} MWCO.

Separation of the Resulting Polymers for IR and Elemental Analyses. The polymers were isolated and purified using the following procedure: the polymer was flocculated by adding 20 mL of methanol to 2 g of suspension and separated by centrifugation (8000 rpm, 15 min). The resulting white precipitate was extensively washed with demineralized water (stirring for 1 h followed by centrifugation) and finally dried at 50 °C (method A). When the polymer was not flocculated by adding methanol, the polymer was isolated by extensive dialysis of the suspension against water (at least 10 times), then by washing the polymer with hot water (200 mL), and finally drying at 50 °C (method B).

General Procedure for the Preparation PAMAM[CO_2H]$_n$. A solution of PAMAM[CO_2CH_3]$_n$ (**1**-($G_{0.5}$) or **3**-($G_{1.5}$)) in HCl (1 M) was stirred 3 days at RT and 3 days at 50 °C until completion of the reaction as monitored by ^{1}H NMR. The solvent was evaporated and the residue formed was dried in vacuum during 24 h.

Synthesis of Acid 2-($G_{0.5}$) PAMAM[CO_2H]$_4$. Starting from PAMAM[CO_2CH_3]$_4$ **1**-($G_{0.5}$) (6 g, 96 mmol) in HCl 1 M (500 mL) the target acid **2**-($G_{0.5}$) was obtained as a yellowish solid (5.4 g, 99%). ^{1}H NMR (300 MHz, DMSO-d_6) was performed at 323 K to improve the resolution, δ (ppm): 2.72−2.88 (m, 12H, H_4 and H_9), 3.18 (m, 4H, H_7), 3.34 (m, 12H, H_3 and H_8), 3.48 (m, 4H, H_6), 3.84 (m, 1H, H_1), 4.08 (dd, 2H, J = 1.6 Hz, J = 7.2 Hz, H_2), 8.51 (t, 2H, J = 3.8 Hz, H_5). ^{13}C NMR (75.5 MHz, DMSO-d_6) δ (ppm): 28.1, 28.4, 29.5, 33.6, 47.9, 48.0, 51.2, 72.8, 81.6, 169.4, 171.3, 171.5. IR (KBr) ν (cm^{-1}): 3237 (NH), 1712 (COOH), 1646, 1558 (CONH). HRMS ESI calcd for $C_{25}H_{42}N_5O_{10}$ [(M + H$^+$)]: 572.2932; found: 572.2930.

Synthesis of Acid 4-($G_{1.5}$) PAMAM[CO_2H]$_8$. Starting from PAMAM[CO_2CH_3]$_8$ **3**-($G_{1.5}$) (2 g, 14 mmol) in HCl 1 M (250 mL) the target acid **4**-($G_{1.5}$) was obtained as a yellowish solid (2.1 g, 100%). ^{1}H NMR (300 MHz, DMSO-d_6) was performed at 323 K to improve the resolution, δ (ppm): 2.75−2.88 (m, 28H, H_4, H_9 and H_{14}), 3.23−3.51 (m, 52H, H_3, H_{6-8} and H_{11-13}), 3.70 (m, 1H, H_1), 4.09 (m, 2H, H_2), 8.49 (m, 6H, H_5 and H_{10}). ^{13}C NMR (75.5 MHz, DMSO-d_6) δ (ppm): 28.2, 28.4, 29.2, 29.5, 33.4, 33.7, 48.0, 48.6, 49.0, 49.2, 51.3, 72.8, 81.7, 169.6, 169.7, 171.4, 171.6. IR (KBr) ν (cm^{-1}): 3223 (NH), 1717 (COOH), 1646, 1556 (CONH). HRMS ESI calcd for $C_{57}H_{98}N_{13}O_{22}$ [(M + H$^+$)]: 1316.6949; found: 1316.6960.

Synthesis of Azide-Functionalized Nanoparticles NP_{N3}. The synthesis of primary reactive chlorobenzyl-functionalized nanoparticles NP_{Cl} was obtained following the previously described procedures.[16] Details of the experimental procedures are provided in the Supporting Information. Azide-coated nanoparticles NP_{N3} were prepared by adding an aqueous solution of sodium azide (2.79 g in 10 mL of water) to 80 g of the freshly prepared crude suspension of NP_{Cl} the pH of which was previously adjusted to 7.5. The resulting suspension was stirred at room temperature for 1 week. The excess of sodium azide was then removed by dialysis through a porous cellulose membrane (MWCO 12000−14000D) toward an aqueous solution of DTAB (15 wt %) leading to a stable translucent aqueous suspension of azide-functionalized nanoparticles (NP_{N3}). Polymer particle content in suspension is 4.46 wt %. The polymer was isolated using method A. Chemical composition: C, 81.95; H, 7.08; N, 1.22% corresponding to an azide content of 0.29 mmol/g of polymer. Mean diameter (QELS): 18 nm (PDI: 0.08). IR (KBr) ν (cm^{-1}): 3084, 3060, 3022, 2922, 2849, 2094, 1602, 1508, 1495, 1450, 1232, 1153, 1065, 1030, 903, 834, 796, 762, 703, 539.

Synthesis of Acid-Terminated PAMAM-Functionalized Nanoparticles NP_PAMAM[CO_2H]$_4$. PAMAM derivative **2**-($G_{0.5}$) (80 mg, 0.140 mmol) was dissolved in 2 mL of water. The solution was added to 10 g of the aqueous suspension of azide-functionalized nanoparticles NP_{N3}. The pH was adjusted to 5.7 by adding NaOH (1M). Then, 2 mL of a freshly prepared aqueous solution of $CuSO_4$ (50 mg, 0.313 mmol) and sodium ascorbate (115 mg, 0.580 mmol) was added; the pH was again adjusted to 5.7. The resulting suspension was stirred at room temperature for 5 days. 76 mg of cyclam was added, and then the suspension was dialyzed against aqueous solution of DTAB (15 to 1.5 wt %). Polymer particle content in suspension is 1.8 wt %. The polymer was isolated using method B. Chemical composition: C, 82.91; H, 7.54; N, 2.72%. Mean diameter (QELS): 20 nm (PDI: 0.005). IR (KBr) ν (cm^{-1}): 3395, 3080, 3056, 3028, 2921, 2852, 2096, 1659, 1598, 1487, 1450, 1369, 1258, 1070, 1025, 899, 829, 797, 756, 698, 535.

Synthesis of PAMAM-Functionalized Nanoparticles NP_PAMAM[CO_2H]$_8$. Prepared using the same procedure as above starting from PAMAM derivative **4**-($G_{1.5}$) (187 mg, 0.142 mmol), 10 g of the aqueous suspension of NP_{N3} and 2 mL of aqueous solution of $CuSO_4$ (50 mg, 0.313 mmol) and sodium ascorbate (115 mg, 0.580 mmol). Polymer particle content in suspension is 1.5 wt %. Chemical composition: C, 81.93; H, 7.67; N, 2.78%. Mean diameter (QELS): 18 nm (PDI: 0.053). IR (KBr) ν (cm^{-1}): 3400, 3082, 3058, 3025, 2922, 2851, 2096, 1653, 1601, 1510, 1493, 1452, 1375, 1266, 1182, 1028, 905, 833, 796, 760, 699, 540.

Synthesis of Dansyl_PAMAM-Functionalized Nanoparticles NP_Dns_PAMAM[CO_2H]$_4$. Dansyl derivative **5** (10 mg, 0.035 mmol) was added to 6 g of the aqueous suspension of acid-terminated PAMAM-functionalized nanoparticles (polymer particle content in suspension is 1.8 wt %). The mixture was stirred at room temperature until complete solubilization of **5** (30 min). Then, 1 mL of a freshly prepared aqueous solution of $CuSO_4$ (19 mg, 0.119 mmol) and sodium ascorbate (44 mg, 0.222 mmol) were added. The resulting suspension was stirred at room temperature for 5 days. 29 mg of cyclam (0.145 mmol) was added, and then the suspension was dialyzed against aqueous solution of DTAB (5 wt %) using an ultrafiltration device (Vivascience, Vivaspin concentrator 20, 50 000 MWCO PES). The process was repeated until no dansyl derivative was detected in the filtrate. The polymer was isolated using method B. Chemical composition: C, 81.03; H, 7.24; N, 2.64; S, 0.63% corresponding to a dansyl and a dendrimer content of 0.20 and 0.11 mmol/g of polymer, respectively. Mean diameter (QELS): 18 nm (PDI: 0.088). IR (KBr) ν (cm^{-1}): 3379, 3082, 3058, 3025, 2922, 2850, 2096, 1668, 1601, 1493, 1452, 1329, 1266, 1145, 1071, 1029, 905, 831, 794, 760, 699, 623, 541.

Synthesis of Dansyl_PAMAM-Functionalized Nanoparticles NP_Dns_PAMAM[CO_2H]$_8$. Prepared using the same procedure as above starting from dansyl derivative **5** (30 mg, 0.104 mmol), 8 g of the aqueous suspension of NP_PAMAM[CO_2H]$_8$, and 1 mL of aqueous solution of $CuSO_4$ (21 mg, 0.132 mmol) and sodium ascorbate (49 mg, 0.247 mmol). 32 mg of cyclam (0.160 mmol) was used at the end of the reaction to sequester the copper. Chemical composition: C, 81.11; H, 7.19; N, 2.87; S, 0.75% corresponding to a dansyl and a dendrimer content of 0.23 and 0.06 mmol/g of polymer, respectively. Mean diameter (QELS): 21 nm (PDI: 0.113). IR (KBr) ν (cm^{-1}): 3392, 3082, 3058, 3025, 2922, 2850, 2096, 1653, 1601, 1510,

1493, 1452, 1329, 1266, 1145, 1071, 1029, 905, 838, 794, 760, 700, 623, 573, 541.

RESULTS AND DISCUSSION

The propargyl-functionalized PAMAM dendrons **1**-($G_{0.5}$) and **3**-($G_{1.5}$) were prepared by a divergent synthesis through a repetitive sequence involving a Michael addition using methyl acrylate and an amidation with ethylenediamine starting from propargylamine according to the previously described method.[25] We then investigated the hydrolysis of the methyl ester terminal groups under the conditions reported in the literature.[28] The reaction was performed with formic acid, and the conversion was monitored by ^{1}H NMR spectroscopy. Regardless of the conditions used (reaction run at room temperature or at 50 °C), the singlet methoxy proton chemical shift is still present in the ^{1}H NMR spectrum, indicating that the reaction is not complete even after a prolonged reaction time. In this regard, we tested the ester hydrolysis using HCl (1 M). The reaction mixture was stirred for 3 days at room temperature and then for three days at 50 °C and was followed by ^{1}H NMR. Under these optimized conditions, acid-terminated dendrons **2**-($G_{0.5}$) and **4**-($G_{1.5}$) were isolated in quantitative yields, and their structures were confirmed by ^{1}H and ^{13}C NMR spectroscopy as well as by IR spectroscopy and HRMS. The hydrolysis of the ester groups of **1**-($G_{0.5}$) and **3**-($G_{1.5}$) is evidenced by the absence of ^{1}H and ^{13}C NMR signals for the methoxy groups (δ_H 3.7 ppm and δ_C 51.0 ppm) along with the downfield shifts of all but the amide protons (Figure 1). Protonation of the tertiary amines of **2**-($G_{0.5}$) and **4**-($G_{1.5}$) probably accounts for the observed deshielding of the methylene and alkyne protons.

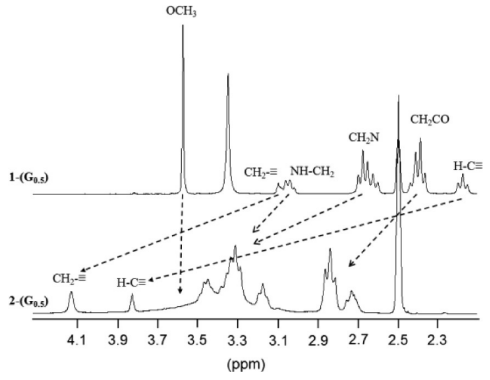

Figure 1. Comparison of ^{1}H NMR spectra of first-generation dendrons **1**-($G_{0.5}$) and **2**-($G_{0.5}$) (in their protonated forms) in DMSO-d_6 at 298 K.

In addition, the IR spectrum of **2**-($G_{0.5}$) shows the expected change in the absorption of the C═O stretching mode from ca. 1729 cm^{-1} for the esters groups to ca. 1712 cm^{-1} for the carboxylic acid moieties. Amide II band, due to NH bending vibrations, also shifts from 1532 cm^{-1} to ca. 1558 cm^{-1} after hydrolysis. Similar results were obtained in the case of second-generation dendron **4**-($G_{1.5}$).

Azido-coated nanoparticles (NP_{N3}) were prepared according to a previously described procedure.[16] In short, reactive benzyl chloride-functionalized nanoparticles (NP_{Cl}) were prepared by copolymerization of styrene, chloromethylstyrene, and divinylbenzene as a cross-linking agent in an oil-in-water microemulsion stabilized with a cationic surfactant (dodecyltrimethylammonium bromide, DTAB). The postfunctionalization reaction was carried out under mild conditions at room temperature by adding an excess of sodium azide (10 equiv per chlorine in the polymer) directly to the nonpurified and freshly prepared aqueous suspension of NP_{Cl}. In aqueous medium, the cross-linked polystyrene-based NPs were not swollen so that the grafting of azide units occurs exclusively on the surface. Unreacted sodium azide was easily removed from the suspension by dialysis at the end of reaction. The presence of azide groups is evidenced by the appearance of the characteristic N_3 stretching band at 2100 cm^{-1} in the IR spectrum (Figure 2a). Elemental analyses confirm this result with an azide load estimated to 0.29 mmol/g of polymer, which corresponds to about 560 N_3 per NP assuming a size of 18 nm for NP_{N3} and a polymer density of 1.05 (Table S1). This simple procedure affords a straightforward access to stable translucent aqueous suspension of azido-coated nanoparticles in the 16−18 nm diameter range. The suspension remained stable when the surfactant concentration was reduced down to 0.15 wt % by dialysis. Unlike the chlorobenzyl-functionalized nanoparticles in which the chlorobenzyl groups are hydrolyzed easily, the azide groups of NP_{N3} are remarkably stable, and the suspension can be stored for more than one year before use. The grafting of the PAMAM dendron was readily performed at room temperature

Scheme 1. Synthesis of Propargyl-Functionalized Acid-Terminated PAMAM Dendrons 2-($G_{0.5}$) and 4-($G_{1.5}$)

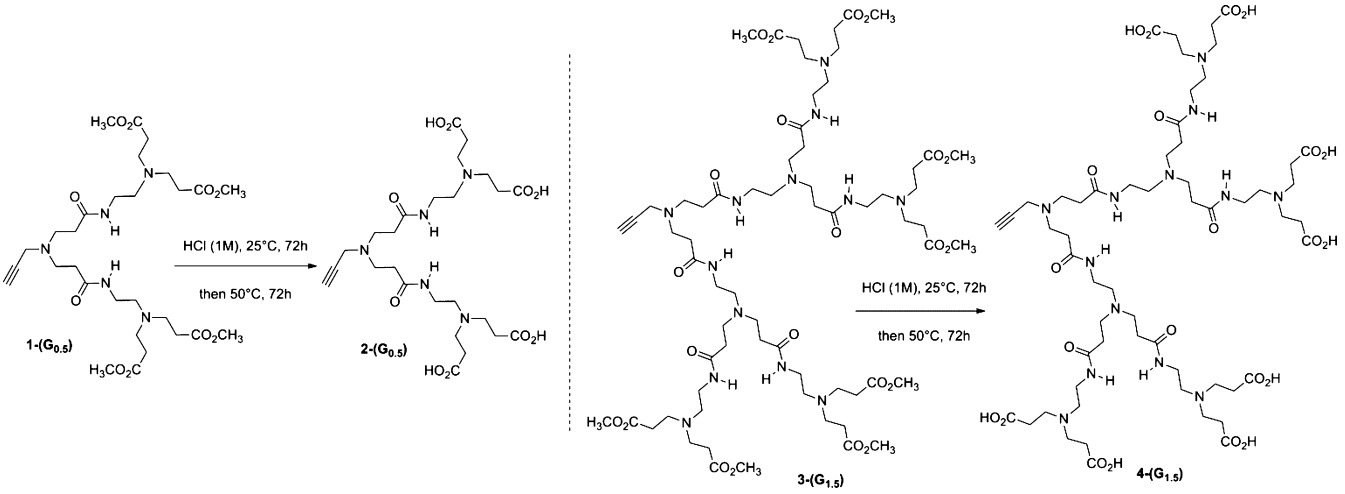

dx.doi.org/10.1021/ma300126h | Macromolecules 2012, 45, 3513−3522

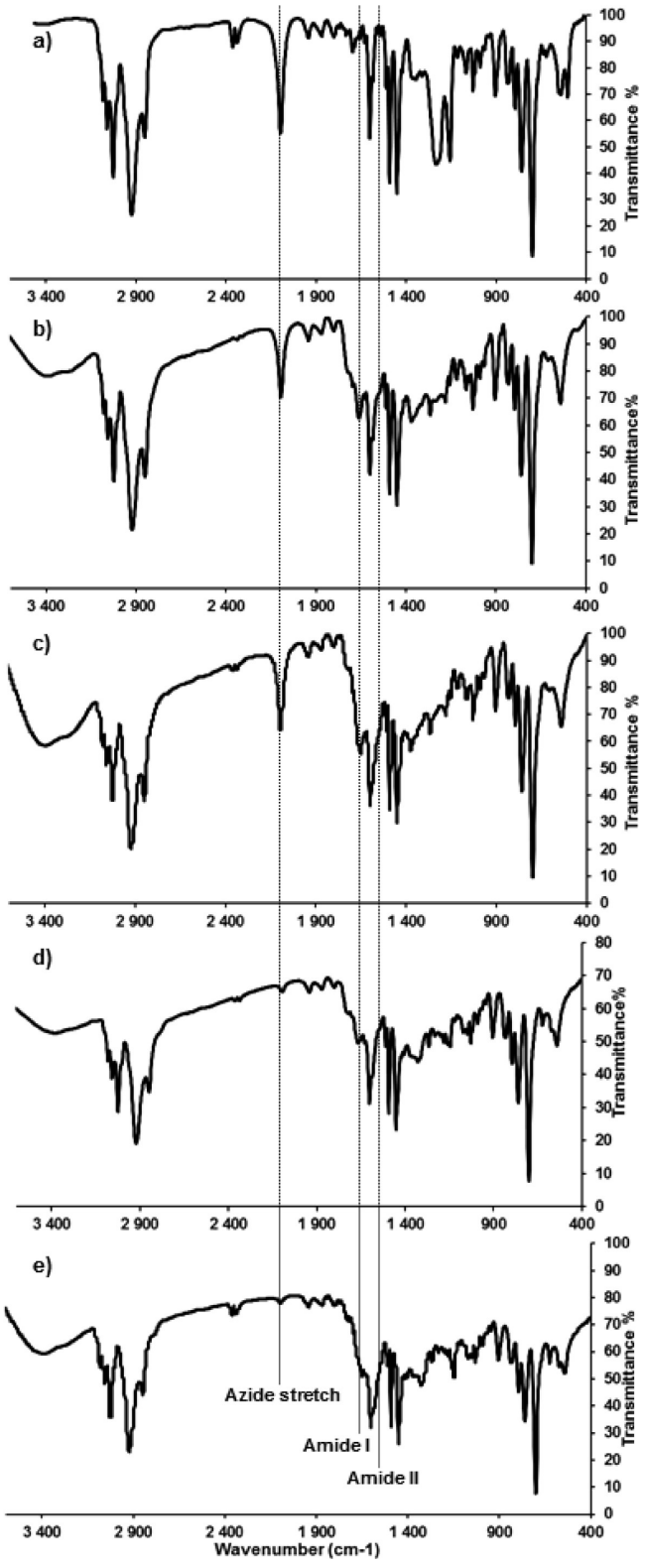

Figure 2. Infrared spectra (a) NP_{N3}, (b) NP_PAMAM$[CO_2H]_4$, (c) NP_PAMAM$[CO_2H]_8$, (d) NP_Dns_PAMAM$[CO_2H]_4$, and (e) NP_Dns_PAMAM$[CO_2H]_8$.

by adding a slight excess of **2**-($\mathbf{G}_{0.5}$) or **4**-($\mathbf{G}_{1.5}$) to the aqueous suspension of azido-coated nanoparticles NP_{N3} using click cycloaddition conditions to provide PAMAM-coated NPs. Owing to the likely affinity of cupric ions for acid-terminated PAMAM dendrons, we used copper sulfate and sodium ascorbate in excess (2.4 and 4.5 equiv, respectively, in relation to the azide content in the polymer) to obtain sufficient content of free copper for the click reaction. At the end of the reaction, cyclam, which has high affinity for cupric ions,[29] was added to easily sequester the excess of copper. The reaction was then purified by exhaustive dialysis against aqueous solutions of DTAB to ensure removal of the cyclam−copper complex, sodium ascorbate, and any unreacted dendrimers. The grafting of PAMAM dendrons on the surface of the nanoparticles can be proved by FT-IR measurement on the isolated and purified polymer (Figure 2b,c). The characteristic absorptions of amide bonds appear at 1660 and 1540 cm^{-1} for amide I and II modes, respectively, although the latter band is superimposed on an aromatic carbon−carbon vibration band. IR spectra also show a decrease of the intensity of the N_3 vibration band at 2100 cm^{-1}, which is more pronounced with **2**-($\mathbf{G}_{0.5}$) than with **4**-($\mathbf{G}_{1.5}$). Elemental analysis is in agreement with these results since nitrogen contents are similar regardless of the generation used (about 1.95 mmol of nitrogen/g of polymer). These facts indicate that the average number of the larger dendron grafted to the NP is lower than that of the smaller dendron. One can assume that the steric hindrance and electrostatic repulsion of the larger dendron ($\mathbf{G}_{1.5}$) are responsible for the lower surface reaction yield for this generation. The availability of unreacted azide groups on the surface of NPs was used as a handle for the attachment of an alkynyl-functionalized dansyl derivative. We have previously reported that the grafting of dansyl on azide-functionalized nanoparticles was almost quantitative using an excess of alkyne dansyl derivative **5** under click conditions.[16] In this work, the reaction was performed in the presence of $CuSO_4$ and sodium ascorbate between 4 equiv of **5** and the remaining azide moieties of the PAMAM-functionalized nanoparticles stabilized with an aqueous solution of 1.5 wt % DTAB, which also ensures the micellar solubilization of the hydrophobic dansyl derivative. After the reaction, exhaustive dialyses were performed to remove the copper catalyst and the unreacted dansyl **5**, until the absence of dye in the filtrate.

The coupling of dansyl was clearly evidenced for both PAMAM dendron-coated NPs by the almost complete disappearance of the azide vibration band in IR spectra of the isolated polymers, indicating a close to quantitative functionalization (Figure 2d,e).

This fact was confirmed by elemental analyses. The amounts of PAMAM and dansyl grafted on the NPs surface, deduced from the nitrogen and sulfur contents of the isolated polymers, were close to the azide content of the starting azide-functionalized nanoparticles (Table 1). One could estimate that the ratio of PAMAM to dansyl moieties grafted on the NPs was around 210/350 and 110/450 for the first and second generation, respectively. These dendron-coated nanoparticles are comparable to high generation PAMAM dendrimers in their functionality with about 840 and 880 peripheral carboxylic acid groups for the first and second generation, respectively.

Using the Mansfield−Tomalia−Rakesh[30] equation (1) for parking spheres on a sphere, the maximum number of dendrons that could be arranged around each nanoparticle was determined to be about 245 and 160 for the first and second generation, respectively.[31]

$$N_{max} = \frac{2\pi}{\sqrt{3}}\left(\frac{r_1}{r_2} + 1\right)^2 \quad (1)$$

dx.doi.org/10.1021/ma300126h | *Macromolecules* 2012, 45, 3513−3522

Scheme 2. Synthesis of Acid-Terminated PAMAM-Functionalized NP_PAMAM$[CO_2H]_n$ and Dansyl-Functionalized NP_Dns_PAMAM$[CO_2H]_n$ Nanoparticles

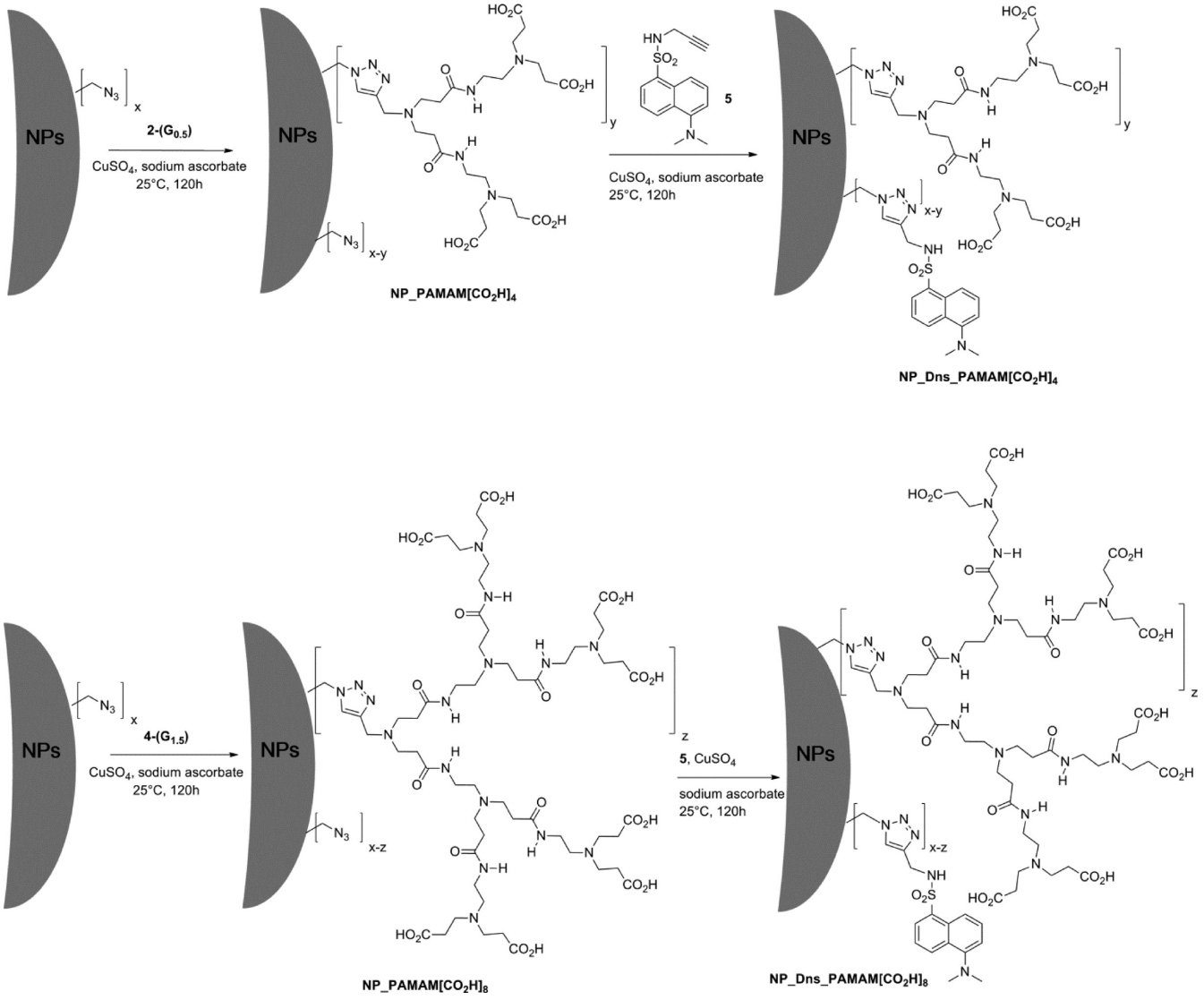

Table 1. Successive Surface Reactions on Azido-Coated Nanoparticles via CuAAC

		NP_PAMAM$[CO_2H]_n$			NP_Dns_PAMAM$[CO_2H]_n$			
list	starting suspension	reactant [x equiv]	D (nm) [PDI][b]	starting suspension	reactant [x equiv]	D (nm) [PDI][b]	PAMAM content[c]	dansyl content[d]
n = 4	NP_{N3}[a]	**2**-($G_{0.5}$) [1.1]	20 [0.005]	NP_PAMAM$[CO_2H]_n$	**5** [4]	18 [0.088]	0.11 (210)	0.20 (350)
n = 8	NP_{N3}[a]	**4**-($G_{1.5}$) [1.1]	18 [0.053]	NP_PAMAM$[CO_2H]_n$	**5** [4]	21 [0.113]	0.06 (110)	0.23 (450)

[a]Azide content in the polymer: 0.29 mmol/g polymer ; D = 18 nm (PDI = 0.08). [b]Particle diameter (D) and its polydispersity index (PDI) determined from QELS. [c]mmol/g of polymer deduced from elemental analysis (nitrogen and sulfur contents). In parentheses: number of PAMAM per NP deduced from the ratio PAMAM/dansyl grafted on the NPs and the content of azide per NP in the starting NP_{N3}. [d]mmol/g of polymer deduced from elemental analysis (nitrogen and sulfur contents). In parentheses: number of dansyl per NP deduced from the ratio PAMAM/dansyl grafted on the NPs and the content of azide per NP in the starting NP_{N3}.

These values, which corroborate fairly well with the experimental results, are indicative of a relatively dense dendritic shell. One can consider that about 85% and 70% of the dendritic shell saturation levels were reached for the first and second generation, respectively. These values are in the same order of magnitude than those obtained by Tomalia et al. in the case of core−shell tecto-dendrimers.[30d] The size and shape of the dendron-grafted NPs were measured in solution using QELS and in the dry state (deposited on a mica substrate) by atomic force microscopy (AFM). The dendron-functionalized NPs have narrow size distributions with mean hydrodynamic diameters of 18−21 nm, as determined by QELS. The dendron-coated NPs exhibit no significant change in diameter and polydispersity relative to the initial NPs (NP_{N3}), thus indicating that the particle size distribution is not modified by the grafting, regardless of the generation of the dendron. Figure 3 shows representative example of AFM image of dendron-functionalized NPs using the tapping mode, which

dx.doi.org/10.1021/ma300126h | Macromolecules 2012, 45, 3513−3522

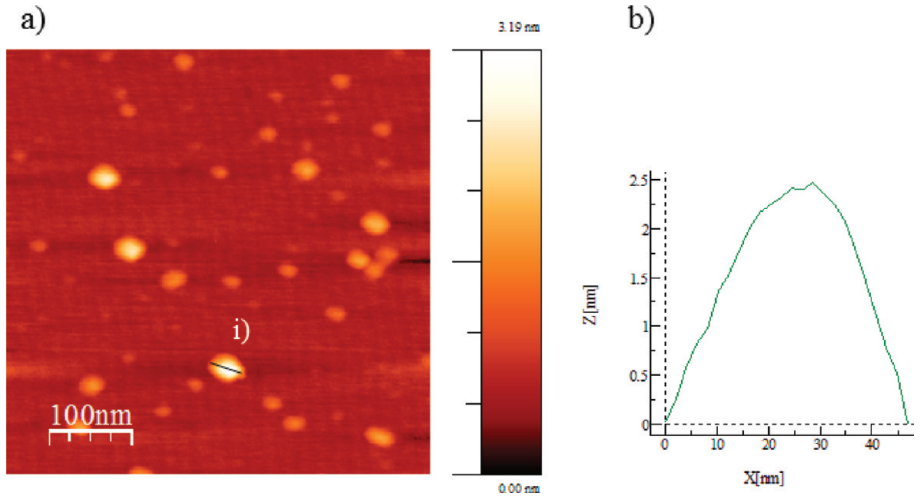

Figure 3. (a) Tapping mode AFM height image of a set of NP_Dns_PAMAM$[CO_2H]_4$ after deposition on a mica substrate. (b) Cross-sectional height profiles corresponding to (i) marked in panel a.

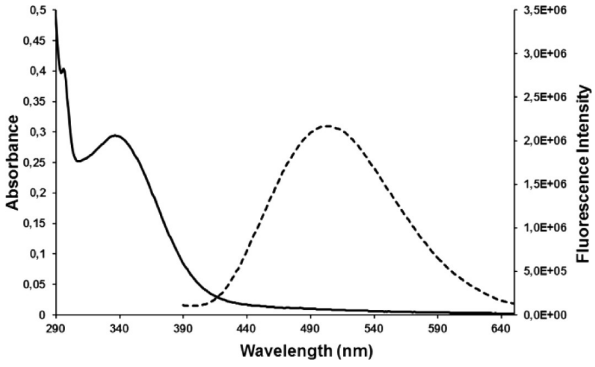

Figure 4. Absorption spectrum (full, 1 wt % DTAB content) and fluorescence emission spectrum (long-dash, λ_{exc} = 336 nm, 0.06 wt % DTAB content) of an aqueous suspension of NP_Dns_PAMAM-$[CO_2H]_4$.

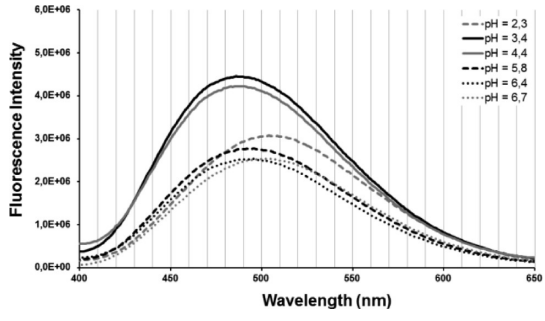

Figure 5. Fluorescence emission spectra of aqueous suspension of NP_dansyl_PAMAM$[CO_2H]_8$ (0.07 wt % DTAB content) for pH values ranging from 2.3 to 6.7. Dansyl was excited at 335 nm.

confirms their spherical morphology. The observation of separate, individual NPs of similar size randomly deposited on the mica surface is indicative of the absence of aggregation. The small height values of the NPs indicate that significant deformation occurs upon adsorption onto the mica AFM surface.[32] Although complicated by the finite size of the AFM tip, the larger lateral sizes of the particles obtained by AFM also supported deformation of the NPs on mica.

The absorption and fluorescence emission spectra of NP_Dns_PAMAM$[CO_2H]_4$ and NP_Dns_PAMAM$[CO_2H]_8$ at neutral pH displayed the characteristic features of dansyl units with a maximum absorption wavelength around 335−340 nm and a broad emission centered around 500 nm (Figure 4 and Figure S3). The blue-shifted emission observed for the dansyl units grafted on the NPs surface relative to the emission bands of dansyl derivatives in water (530−580 nm) indicates that the microenvironment of the dansyl moieties linked to the NP surface is less polar than a surrounding aqueous phase.[33,34] Furthermore, the position of the fluorescence emission band as well as the intensity varied significantly from 485 to 510 nm with changes of pH in the range of 2−7 (Figure 5 and Figures S6 and S7) while the absorption band did not varied. It is well-known that the fluorescence emission position and intensity of dansyl are strongly dependent on the polarity of the medium.[33,35] One may consider that the protonation of PAMAM dendrons induces a change in the local polarity close to the dansyl units to explain this result.

The colloidal stability of acid-terminated dendron-functionalized nanoparticles NP_PAMAM$[CO_2H]_n$ was first studied by decreasing the content of surfactant in the suspension in order to assess if the dendron shell could act as a protective layer and permit the stabilization of nanoparticles in surfactant free suspensions as already observed in dendritic-coated polymeric nanoparticles.[21,22] Experimental details of nanoparticles NP_PAMAM$[CO_2H]_n$-bis used for this study are provided in the Supporting Information. When the surfactant concentration was close to 0.3 wt % and the pH to 7, the aggregation of nanoparticles took place regardless of the grafted dendron while the initial nanolatexes (NP_{N3}) remained stable at this concentration (vide supra). This result suggests that the formation of ion pairs between ammonium moieties of DTAB and carboxylate groups of PAMAM dendrons occurs. This type of interaction has already been reported by Tomalia between PAMAM dendrimers and dodecylammonium bromide leading to generation-dependent surfactant aggregates.[36] The surfactant molecules self-assemble at the nanoparticle surface orienting their hydrophobic chains toward the aqueous solution, which leads to a colloidal destabilization of the suspension. Then, the colloidal stability of PAMAM dendron-coated NPs was assessed both in acidic and basic media (Figure 6). The experiment were performed in the presence of DTAB since the dialysis of dendron-coated nanoparticles against acidic

dx.doi.org/10.1021/ma300126h | Macromolecules 2012, 45, 3513−3522

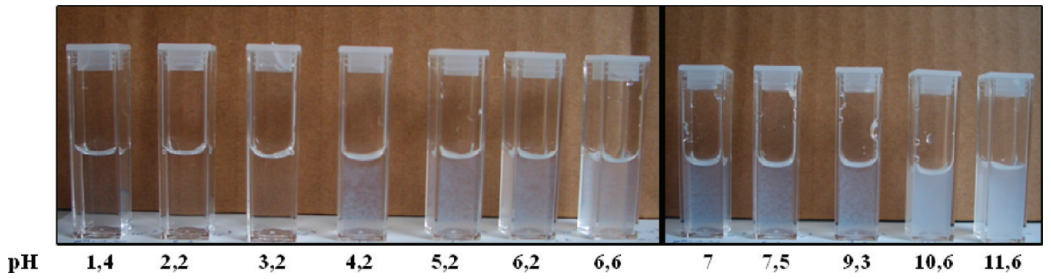

Figure 6. Pictures depicting the colloidal stability of NP_PAMAM$[CO_2H]_8$-bis versus pH.

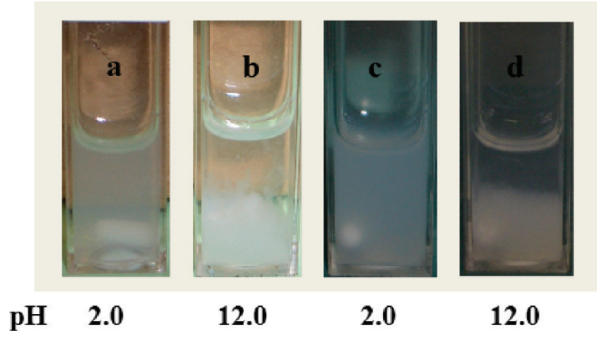

Figure 7. Photographs of NP_PAMAM$[CO_2H]_4$-bis (0.02 wt % DATB content) after standing 24 h: from the starting suspension (initial pH 2.0) after the first sequence final pH 2.0 (a), solution from (a) after basification pH 12.0 (b), from the starting suspension after three sequences final pH 2.0 (c), solution from (c) after basification pH 12.0 (d).

solution (pH = 2) led to the formation of hydrogel. The suspensions stabilized with 1.0 wt % of DTAB were diluted 50 times in HCl (concentrations range from 6×10^{-2} to 6×10^{-7} M) or in NaOH (concentrations range from 6×10^{-2} to 6×10^{-7} M). The suspensions of dendron-grafted NPs are stable at pH $\leq$ 3.2 regardless of the dendron generation. The pK_a values of internal tertiary amines moieties for PAMAM dendrimer are between 6.0 and 7.3.[37] At pH = 3, all the tertiary amines and carboxylic groups are protonated. The PAMAM dendron grafted to the surface of NPs could be assumed to be mainly in the protonated form at this pH, thus ensuring along with the remaining DTAB an electrostatic stabilization of the colloidal suspensions. So one could assume that, at acidic pHs ($\leq$3.2), the stabilization of the suspensions by electrostatic repulsions was kept and led to translucent suspension. Moreover, the size of the nanoparticles in acidic medium was not modified and was found to be in the 15−20 nm diameter range.

When the pH increased from 4 to 12, the suspensions turned cloudy and the polymer precipitated. Considering a pK_a value close to 4 for carboxylic acid groups,[38] the formation of ion pairs between ammonium units and carboxylate groups can be envisioned which leads to the immediate aggregation and precipitation of the nanoparticles. The reversibility of the electrostatic self-assembly process was then studied (Figure 7). The experiment was run on the previous diluted suspension using hydrochloric acid or sodium hydroxide to adjust the pH. The starting suspension (pH = 2) was basified then acidified (first sequence) and led to a cloudy aqueous suspension (as shown in Figure 7a) without precipitation of the polymer even after standing for 2 weeks (see Figure S10). This result indicates that some nanoparticles aggregate but that the overall charge on the resulting particles is large enough to prevent precipitation. This base−acid sequence process has been repeated three times and led to the same observation: polymer particles precipitated in basic medium after standing for 24 h and could be redispersed in acidic medium regardless of the generation. The sizes of the particles were determined at pH = 2 by QELS at the end of the three sequences. The resulting suspension of particle were polydisperse; the size of particles were found to be about 170 and 760 nm for NP_PAMAM-$[CO_2H]_4$-bis and 360 and 960 nm for NP_PAMAM$[CO_2H]_8$-bis. The precipitation of the polymer in basic medium does not allow the measurement of the hydrodynamic diameter by DLS analysis.

Although the initial size of the nanoparticles was altered, this reversible switchability would confer striking benefits, implying for instance the possible separation and redispersion of the polymeric particles. Furthermore, in agreement with a steric stabilization from the dendritic shell, aqueous suspensions of dendron-coated nanoparticles tolerated the addition of ethanol and remained stable up to 9:1 ethanol/water volumes regardless of the generation, while the initial nanolatex (NP_{N3}) suspension precipitated upon addition of ethanol.

CONCLUSION

This study demonstrates that azido-coated polymer nanoparticles (NP_{N3}) obtained by the postfunctionalization procedure can be used as a clickable platform for the convergent synthesis of fluorescent polystyrene core−PAMAM shell nanoparticles in the 15−20 nm diameter range. Owing to the nonswelling properties of cross-linked polystyrene matrix in water and to the fact that azide units are located only the surface, the grafting of PAMAM dendron and dansyl derivative occurs exclusively on the NP_{N3} surface. The reaction was particularly efficient with almost quantitative overall yield. The reaction proceeded under very mild conditions using $CuSO_4$ and sodium ascorbate as a catalytic system. The whole process was achieved in water without any added cosolvent in the presence of the surfactant which allowed the micellar solubilization of hydrophobic dansyl derivative. Remarkably, the use of earlier generation of PAMAM dendron ($\mathbf{G_{0.5}}$ and $\mathbf{G_{1.5}}$) allows the preparation in a few steps of dendron-coated nanoparticles which possess properties comparable to high eighth generation of PAMAM dendrimers in their functionality[39] and to core−shell tecto-dendrimer in their size.[40] Dendritic shell saturations levels of 85% and 70% were reached for the first and second generation, respectively. Dendron-coated nanoparticles can be considered as multifunctional systems composed of (i) an interior of shell with azide groups remaining after the grafting of PAMAM dendrons and located onto the NPs surface and (ii) an outer shell with peripheral carboxylic acid moieties. This approach allows the control of both the location and the distribution of a given

dx.doi.org/10.1021/ma300126h | Macromolecules 2012, 45, 3513−3522

chemical group in each part of the shell which carries out its designed task. This has been demonstrated by grafting of fluorescent dansyl derivative in the interior of shell. As far as peripheral carboxylic acid moieties are concerned, surface functionalization with various molecules (biomolecules or fluorescent dyes) can be envisioned via ion pair association or covalent linkages and are currently under investigation in our laboratory. Finally, the strategy presented here is quite general and should give a straightforward access to a variety of dendron-coated nanoparticles, thereby opening new perspectives in the field of materials science and biotechnology.

■ ASSOCIATED CONTENT

Supporting Information

Additional structures of **2-G**$(_{0.5})$ and **4-**$(\mathbf{G}_{1.5})$, experimental procedures, spectral characterization data, figures, and tables. This material is available free of charge via the Internet at http://pubs.acs.org.

■ AUTHOR INFORMATION

Corresponding Author

*E-mail: Emmanuel.Allard@chimie.uvsq.fr.

Notes

The authors declare no competing financial interest.

■ ACKNOWLEDGMENTS

M.C. thanks Fundacion Progreso y Salud (Ministry of Health from Junta de Andalucía) for the financial support through a Postdoctoral fellowship in Nanomedicine 2010−2012 (ref 0399). M.C. and E.A. thank B. Berrini for helpful assistance with the AFM measurements.

■ REFERENCES

(1) (a) Goesmann, H.; Feldmann, C. *Angew. Chem., Int. Ed.* **2010**, *49*, 1362−1395. (b) Shipway, A. N.; Katz, E.; Willner, I. *ChemPhysChem* **2000**, *1*, 18−52.

(2) De, M.; Ghosh, P. S.; Rotello, V. M. *Adv. Mater.* **2008**, *20*, 4225−4241.

(3) Astruc, D.; Lu, F.; Aranzaes, J. R. *Angew. Chem., Int. Ed.* **2005**, *44*, 7852−7872.

(4) Aiken, J. D.; Finke, R. G. *J. Mol. Catal. A: Chem.* **1999**, *145*, 1−44.

(5) Bronstein, L. M.; Shifrina, Z. B. *Chem. Rev.* **2011**, *111*, 5301−5344.

(6) *Dendrimers and Dendrons: Concepts, Syntheses, Applications*; Newkome, G. R., Moorefield, C. N., Voegtle, F., Eds.; Wiley-VCH: Weinheim, 2001.

(7) *Dendrimers and Other Dendritic Polymers*; Fréchet, J., Tomalia, D., Eds.; Wiley: Chichester, UK, 2001.

(8) (a) Crooks, R. M.; Zhao, M.; Sun, L.; Chechik, V.; Yeung, L. K. *Acc. Chem. Res.* **2001**, *34*, 181−190. (b) Astruc, D.; Boisselier, E.; Ornelas, C. *Chem. Rev.* **2010**, *110*, 1857−1959. (c) Vohs, J. K.; Fahlman, B. D. *New J. Chem.* **2007**, *31*, 1041−1051.

(9) (a) Guo, W.; Li, J. J.; Wang, A.; Peng, X. *Chem. Mater.* **2003**, *15*, 3125−3133. (b) Guo, W.; Li, J. J.; Wang, A.; Peng, X. *J. Am. Chem. Soc.* **2003**, *125*, 3901−3909. (c) Advincula, R. C. *Dalton Trans.* **2006**, 2778−2784. (d) Cutler, E. C.; Lundin, E.; Garabato, B. D.; Choi, D.; Shon, Y.-S. *Mater. Res. Bull.* **2007**, *42*, 1178−1185. (e) Danda, C.; Ponnapati, R.; Dutta, P.; Taranekar, P.; Patterson, G.; Advincula, R. C. *Macromol. Chem. Phys.* **2011**, *212*, 1600−1615. (f) Zhou, D.; Li, Y.; Hall, E. A. H.; Abell, C.; Klenerman, D. *Nanoscale* **2011**, *3*, 201−211. (g) Daniel, M.-C.; Grow, M. E.; Pan, H.; Bednarek, M.; Ghann, W. E.; Zabetakis, K.; Cornish, J. *New J. Chem.* **2011**, *35*, 2366−2374.

(10) (a) Mizugaki, T.; Murata, M.; Fukubayashi, S.; Mistudome, T.; Jitsukawa, K.; Kaneda, K. *Chem. Commun.* **2008**, 241−243. (b) Love, C. S.; Chechik, V.; Smith, D. K.; Brennan, C. *J. Mater. Chem.* **2004**, *14*, 919−923. (c) Gopidas, K. R.; Whitesell, J. K.; Fox, M. A. *J. Am. Chem. Soc.* **2003**, *125*, 6491−6502. (d) Jiang, G.; Wang, L.; Chen, T.; Yu, H.; Wang, J. *Nanotechnology* **2004**, *15*, 1716−1719. (e) Wang, R.; Yang, J.; Zheng, Z.; Carducci, M. D.; Jiao, J.; Seraphin, S. *Angew. Chem., Int. Ed.* **2001**, *40*, 549−552.

(11) (a) Heuzé, K.; Rosario-Amorin, D.; Nlate, S.; Gaboyard, M.; Bouter, A.; Clérac, R. *New J. Chem.* **2008**, *32*, 383−387. (b) Rosario-Amorin, D.; Wang, X.; Gaboyard, M.; Clérac, R.; Nlate, S.; Heuzé, K. *Chem.—Eur. J.* **2009**, *15*, 12636−12643. (c) Moussodia, R.-O.; Balan, L.; Merlin, C.; Mustin, C.; Schneider, R. *J. Mater. Chem.* **2010**, *20*, 1147−1155. (d) Kainz, Q. M.; Schätz, A.; Zöpfl, A.; Stark, W. J.; Reiser, O. *Chem. Mater.* **2011**, *23*, 3606−3613.

(12) (a) Pichot, C. *Curr. Opin. Colloid Interface Sci.* **2004**, *9*, 213−221. (b) Antonietti, M.; Tauer, K. *Macromol. Chem. Phys.* **2003**, *204*, 207−219.

(13) (a) Kunna, K.; Müller, C.; Loos, J.; Vogt, D. *Angew. Chem., Int. Ed.* **2006**, *45*, 7289−7292. (b) Mohammed, H. S.; Shipp, D. A. *Macromol. Rapid Commun.* **2006**, *27*, 1774−1778. (c) Voorn, D.-J.; Ming, W.; Herk, A. M. V. *Macromolecules* **2005**, *38*, 3653−3662. (d) Castelvetro, V.; Vita, C. D. *Adv. Colloid Interface Sci.* **2004**, *108−109*, 167−185. (e) Ford, W. T. *React. Funct. Polym.* **1997**, *33*, 147−158.

(14) (a) Amigoni-Gerbier, S.; Larpent, C. *Macromolecules* **1999**, *32*, 9071−9073. (b) Amigoni-Gerbier, S.; Désert, S.; Gulik, T.; Larpent, C. *Macromolecules* **2002**, *35*, 1644−1650. (c) Méallet-Renault, R.; Pansu, R.; Amigoni-Gerbier, S.; Larpent, C. *Chem. Commun.* **2004**, 2344−2345. (d) Cannizzo, C.; Amigoni-Gerbier, S.; Larpent, C. *Polymer* **2005**, *46*, 1269−1276. (e) Gouanvé, F.; Schuster, T.; Allard, E.; Méallet-Renault, R.; Larpent, C. *Adv. Funct. Mater.* **2007**, *17*, 2746−2756. (f) Allard, E.; Larpent, C. *J. Polym. Sci., Part A: Polym. Chem.* **2008**, *46*, 6206−6213. (g) Abid, J.-P.; Frigoli, M.; Pansu, R.; Szeftel, J.; Zyss, J.; Larpent, C.; Brasselet, S. *Langmuir* **2011**, *27*, 7967−7971. (h) Zhu, L.; Wu, W.; Zhu, M.-Q.; Han, J. J.; Hurst, J. K.; Li, A. D. Q. *J. Am. Chem. Soc.* **2007**, *129*, 3524−3526. (i) Tian, Z.; Shaller, A. D.; Li, A. D. Q. *Chem. Commun.* **2009**, 180−182. (j) Sun, H.; Almdal, K.; Andrese, T. L. *Chem. Commun.* **2011**, *47*, 5268−5270.

(15) (a) Larpent, C.; Tadros, C. F. *Colloid Polym. Sci.* **1991**, *269*, 1171−1183. (b) Antonietti, M.; Basten, R.; Lohmann, S. *Macromol. Chem. Phys.* **1995**, *196*, 441−466. (c) Hentze, H. P.; Kaler, E. W. *Curr. Opin. Colloid Interface Sci.* **2003**, *8*, 164−178. (d) Larpent, C. In *Surfactant Science Series, Colloid Polymers: Preparation and Biomedical Applications*; Elaissari, A., Ed.; Marcel Dekker: New York, 2003; Vol. *115*, Chapter 7, pp 145−187. (e) Yan, F.; Texter, J. *Soft Matter* **2006**, *2*, 109−118.

(16) Ouadahi, K.; Allard, E.; Oberleitner, B.; Larpent, C. *J. Polym. Sci., Part A: Polym. Chem.* **2012**, *50*, 314−328.

(17) Wesler, K.; Perera, M. D. A.; Aylott, J. W.; Chan, W. C. *Chem. Commun.* **2009**, 6601−6603.

(18) (a) Joralemon, M. J.; O'Reilly, R. K.; Hawker, C. J.; Wooley, K. L. *J. Am. Chem. Soc.* **2005**, *127*, 16892−16899. (b) O'Reilly, R. K.; Joralemon, M. J.; Hawker, G. J.; Wooley, K. L. *New J. Chem.* **2007**, *31*, 718−724.

(19) (a) Li, B.; Martin, A. L.; Gillies, E. R. *Chem. Commun.* **2007**, 5217−5219. (b) Martin, A. L.; Li, B.; Gillies, E. R. *J. Am. Chem. Soc.* **2009**, *131*, 734−741.

(20) Nazemi, A.; Amos, R. C.; Bonduelle, C. V.; Gillies, E. R. *J. Polym. Sci., Part A: Polym. Chem.* **2011**, *49*, 2546−2559.

(21) Larpent, C.; Geniès, C.; De Souza Delgado, A. P.; Caminade, A.-M.; Majoral, J.-P.; Sassi, J.-F.; Leising, F. *Chem. Commun.* **2004**, 1816−1817.

(22) (a) Larpent, C.; Cannizzo, C.; Delgado, A.; Gouanvé, F.; Sanghvi, P.; Gaillard, C.; Bacquet, G. *Small* **2008**, *4*, 833−840. (b) Cannizzo, C.; Amigoni-Gerbier, S.; Frigoli, M.; Larpent, C. *J. Polym. Sci., Part A: Polym. Chem.* **2008**, *46*, 3375−3386.

(23) Tornøe, C. W.; Christensen, C.; Meldal, M. *J. Org. Chem.* **2002**, *67*, 3057−3064.

(24) Rostovtsev, V. V.; Green, L. G.; Fokin, V. V.; Sharpless, K. B. *Angew. Chem., Int. Ed.* **2002**, *41*, 2596−2599.

(25) (a) Lee, J. W.; Kim, B.-K.; Kim, J. H.; Shin, W. S.; Jin, S.-H. *J. Org. Chem.* **2006**, *71*, 4988−4991. (b) Lee, J. W.; Kim, B.-K.; Kim, H. J.; Han, S. C.; Shin, W. S.; Jin, S.-H. *Macromolecules* **2006**, *39*, 2418−2422. (c) Lee, J. W.; Kim, H. J.; Han, S. C.; Kim, J. H.; Jin, S.-H. *J. Polym. Sci., Part A: Polym. Chem.* **2008**, *46*, 1083−1097.
(26) Gottlieb, H. E.; Kotlyar, V.; Nudelman, A. *J. Org. Chem.* **1997**, *62*, 7512−7515.
(27) Horcas, I.; Fernández, R.; Gómez-Rodriguez, J. M.; Colchero, J.; Gómez-Herrero, J.; Baro, A. M. *Rev. Sci. Instrum.* **2007**, *78*, 013705−1-013705−6.
(28) Tulu, M.; Aghatabay, N. M.; Senel, M.; Dizman, C.; Parali, T.; Dulger, B. *Eur. J. Med. Chem.* **2009**, *44*, 1093−1099.
(29) Thöm, V. J.; Hosken, G. D.; Hancock, R. D. *Inorg. Chem.* **1985**, *24*, 3378−3381.
(30) (a) Mansfield, M. L.; Rakesh, L.; Tomalia, D. A. *J. Chem. Phys.* **1996**, *105*, 3245−3249. (b) Tomalia, D. A. *Prog. Polym. Sci.* **2005**, *30*, 294−324. (c) Jensen, A. W.; Maru, B. S.; Zhang, X.; Mohanty, D. K.; Fahlman, B. D.; Swanson, D. R.; Tomalia, D. A. *Nano Lett.* **2005**, *5*, 1171−1173. (d) Uppuluri, S.; Swanson, D. R.; Piehler, L. T.; Li, J.; Hagnauer, G. L.; Tomalia, D. A. *Adv. Mater.* **2000**, *12*, 796−800.
(31) Equation 1; $r_1/r_2 > 1.20$, r_1 is the nanoparticle radius of starting azide-functionalized nanoparticles (determined from QELS). Even if the dendrons does not adopt a spherical geometry, one can estimate the radii of **2**-($\mathbf{G}_{0.5}$) (r_2 = 1.25 nm) and **4**-($\mathbf{G}_{1.5}$) (r_2 = 1.6 nm) considering that the dendrons have an extended conformation without correction for charge, solvation, etc., using Chem Bio3D Ultra 11.0 (MM2 calculation) software (Supporting Information, Figure S11).
(32) (a) Betley, T. A.; Hessler, J. A.; Mecke, A.; Banaszak Holl, M. M.; Orr, B. G.; Uppuluri, S.; Tomalia, D. A.; Baker, J. R., Jr. *Langmuir* **2002**, *18*, 3127−3133. (b) Dukette, T. F.; Mackay, M. E.; Van Horn, B.; Wooley, K. L.; Drockenmuller, E.; Malkoch, M.; Hawker, C. J. *Nano Lett.* **2005**, *5*, 1704−1709.
(33) (a) Nelissen, H. F. M.; Venema, F.; Uittenbogaard, R. M.; Feiters, M. C.; Nolte, R. J. M. *J. Chem. Soc., Perkin Trans. 2* **1997**, 2045−2053. (b) Montalti, M.; Prodi, L.; Zaccheroni, N.; Battistini, G.; Marcuz, S.; Mancin, F.; Rampazzo, E.; Tonellato, U. *Langmuir* **2006**, *22*, 5877−5881.
(34) Ouadahi, K.; Sbargoud, K.; Allard, E.; Larpent, C. *Nanoscale* **2012**, DOI: 10.1039/C2NR11413E.
(35) Wang, B.-B.; Zhang, X.; Jia, X.-R.; Li, Z.-C.; Ji, Y.; Yang, L.; Wei, Y. *J. Am. Chem. Soc.* **2004**, *126*, 15180−15194.
(36) Caminati, G.; Turro, N. J.; Tomalia, D. A. *J. Am. Chem. Soc.* **1990**, *112*, 8515−8522.
(37) (a) Cakara, D.; Kleimann, J.; Borkovec, M. *Macromolecules* **2003**, *36*, 4201−4207. (b) Diallo, M. S.; Christie, S.; Swaminathan, P.; Balogh, L.; Shi, X.; Um, W.; Papelis, C.; Goddard, W. A., III; Johnson, J. H., Jr. *Langmuir* **2004**, *20*, 2640−2651. (c) Kannaiyan, D.; Imae, T. *Langmuir* **2009**, *25*, 5282−5285.
(38) Van Duijvenbode, R. C.; Rajanayagam, A.; Koper, G. J. M.; Baars, M. W. P. L.; De Waal, B. F. M.; Meijer, E. W.; Borkovec, M. *Macromolecules* **2000**, *33*, 46−52.
(39) Sharma, A.; Desai, A.; Ali, R.; Tomalia, D. A. *J. Chromatogr., A* **2005**, *1081*, 238−244.
(40) Li, J.; Swanson, D. R.; Qin, D.; Brothers, H. M.; Piehler, L. T.; Tomalia, D. A.; Meier, D. J. *Langmuir* **1999**, *15*, 7347−7350.